The mean-field Hubbard model for bosons in complex networks

Paulo Cesar Ventura da Silva

Instituto de Física de São Carlos, Universidade de São Paulo,
Avenida Trabalhador São Carlense 400, Caixa Postal 369,
CEP 13560-970, São Carlos, São Paulo, Brazil

(Dated: November 27, 2018)

Several physical models have been studied in complex networks, which have proven to modify their critical behavior and produce new phenomenology. We study the Bose-Hubbard model in complex networks of sites under mean-field hypothesis. We apply numerical methods to draw the phase diagram for annealed and quenched scale-free networks. We also use an analytical approach to predict the mean-field quantum phase transition between a Mott insulator and a superfluid phase. In agreement with previous findings in other models, we show that the critical point vanishes at the thermodynamic limit, for annealed networks with diverging second degree moment and for quenched networks with diverging maximum degree. Moreover, for the quenched case, we show how the local superfluid activity correlates with the centrality of the sites. Despite the limitations of the mean-field approximation, we argue that our results indicate the absence of a Mott insulating phase for large scale-free populations of sites.

I. INTRODUCTION

Over the last two decades, the study of dynamic processes and physical models in complex networks became very popular in the scientific community [1–4], considerably improving our understanding on how the heterogeneity and complexity of contacts in structured populations affect processes that run over them. Despite some marginal development occurred over the 20th century, the science of complex systems was mainly developed after the discovery, in the late 90's, that most real-world networks share some common properties, such as a scale-free degree distribution [5] and the small-world property [6].

The body of research in complex systems have been mainly developed over biological, social and technological systems, such as protein [7] and biomolecular [8] networks, social media an propagation of information [9–11], epidemic spreading [12–14], power grids [15] and many other examples. However, considerable attention have also been driven to physical problems in complex networks, such as the Ising model [16, 17], the Anderson localization [18, 19], the XY model [20], spin-1/2 Hubbard model [21] and Bose-Einstein condensation [22–24].

Critical phenomena are very often found in such systems, and the structure of the network may have a crucial influence over them. It has been shown that the degree distribution (in particular, the second degree moment $\langle k^2 \rangle$)) and the spectrum of the adjacency matrix have strong influence in the critical behavior of the Ising model [17], synchronization models [25], epidemic spreading [12] and the percolation process [26]. As an illustration, Burioni *et al.* [22] shows that the inhomogeneous structure of a complex network can induce a Bose-Einstein condensation even in systems with low dimension ($d \leq 2$) and non-interacting bosons, a behavior that is not observed in regular lattices. This happens due to anomalies in the density of states, and the phenomenon is known as "topology-induced Bose-Einstein condensation". Another example is the critical temperature enhancement

of the superconducting phase transition using a scale-free topology in the Random Transverse Ising model [27]. A review of critical phenomena in complex networks can be found in ref. [28].

The new phenomenology of physical models in complex networks have potential applications for technological purposes and basic physics development. Optical lattices [29, 30] have been successfully used to experimentally reproduce theoretical predictions of condensed matter systems [31] using ultracold atoms. More recently, the production of arbitrary optical potentials [32–34] opens the possibility of simulating more complex quantum systems, including heterogeneous contact topologies. The combination of experimental and theoretical efforts in this direction may give rise to important applications, such as using the topology of sites to tune the critical behavior of the system.

In this work, we study the Bose-Hubbard model in complex networks in a mean-field framework. We study the influence of a heterogeneous structure of contacts in the model, giving particular attention to the scale-free configuration. A scale-free network is such that the connectivity of the nodes (sites) follows a power-law distribution $P(k) \propto k^{-\alpha}$. We show that, similarly to the epidemic onset in the SIS model [12], the ferromagnetic transition in Ising model [17] and the percolation threshold [26], the transition between the Mott insulator and the superfluid phases has a vanishing critical point at the thermodynamic limit for networks with power-law exponent $\alpha \leq 3$. We apply the model for two different network formulations - the annealed and quenched - and discuss the differences between each formulation for scale-free networks. We study the local site activity information given by the quenched formulation, and compare the activity with the centrality of each site. Finally, we present a brief discussion about the Bose glass phase, which cannot be predicted by mean-field theory, but is important to correctly understand the meaning of the vanishing phase transition.

The paper is structured as follows: section II briefly presents the mean-field formulation of the Bose-Hubbard model. The equations are further developed in sections III and IV, in which we present respectively the annealed and the quenched formulations. In each of these two sections, we compute the site-decoupled Hamiltonian, calculate the insulator/superfluid critical point and compare with numerical simulations. In section IV C, we also discuss some results with the local field. In section V, we discuss limitation of the mean-field approach and its consequence for the interpretation of our results.

II. BOSE-HUBBARD MODEL IN THE MEAN-FIELD APPROACH

The Bose-Hubbard model [35] is a simple and powerful description for interacting bosons trapped in a set of confining potential wells (sites). It can be experimentally implemented in optical lattices [36, 37], and presents rich phenomenology with a relatively small number of parameters. The Bose-Hubbard Hamiltonian for spinless bosons accounts for local boson-boson interactions and nearest neighboring site tunnelling, and can be written as:

$$\hat{H} = \sum_i \left\{ \frac{U}{2} n_i(n_i - 1) - \mu n_i \right\} - t \sum_{i,j} \alpha_{ij} a_i a_j^\dagger \quad (1)$$

where i and j are indexes that run over the nodes (sites) of the network, and the adjacency matrix α_{ij} is such that $\alpha_{ij} = 1$ if nodes i and j are connected and $\alpha_{ij} = 0$ otherwise. For this work, we consider undirected graphs, meaning that the adjacency matrix is symmetric (therefore, the *h.c.* of $a_i a_j^\dagger$ is present on the sum by exchanging indexes). The operators $a_i^\dagger$ and a_i are respectively the creator and annihilator of spinless bosons at site i, and $n_i = a_i^\dagger a_i$ is the number operator for bosons at that site. The on-site boson-boson interactions are represented by parameter U, and the hopping between nearest neighboring ha amplitude given by parameter t. The system can accept particles from or reject particles to a reservoir, depending on the chemical potential μ.

At zero-temperature, and in the limit of no interaction ($U \ll t, \mu$), the bosons move independently over the network, and the system presents a superfluid behavior. On the other hand, for the limit of strong interactions or weak hopping ($U, \mu \gg t$), the Hamiltonian is diagonal on the particle number basis, and the bosons are uniformly distributed over the sites in order to minimize the energy, forming a Mott insulator. Using a mean-field approach, we are able to study the model for intermediate values of the parameters, and therefore capture the transition between the Mott insulator and superfluid phase. Moreover, the mean-field approach allows for easily studying the Bose-Hubbard model for more general

connection patterns than the regular lattice, such as a complex network.

We follow the standard mean-field approach used for the Bose-Hubbard model [38–40], generalizing it for an arbitrary connection pattern (adjacency matrix α_{ij}). In this mean-field approximation, the hopping term can be site-decoupled by making:

$$
\begin{aligned}
a_i^\dagger a_j &\approx \langle a_i^\dagger \rangle a_j + \langle a_j \rangle a_i^\dagger - \langle a_i^\dagger \rangle \langle a_j \rangle \\
&\approx \psi_i^* a_j + \psi_j a_i^\dagger - \psi_i^* \psi_j \quad (2)
\end{aligned}
$$

Where $\psi_i = \langle a_i \rangle$ and $\psi_i^* = \langle a_i^\dagger \rangle$. ψ_i is the superfluid parameter for site i, which we shall often refer as *field*. Despite, in principle, the field ψ_i is complex, we can capture the desired phenomenology by assuming it is a real variable, i.e., $\psi_i^* = \psi_i$, $\forall i = 1, 2, ..., N$ - an assumption that simplifies the numerical analysis.

Under the mean-field assumption (eq. 2), the total Hamiltonian is decoupled in single-site non-interacting components plus an overall term, with both depending on the field $\{\psi_i\}$. The order parameter can be determined self-consistently by minimizing the free energy, which for $T = 0$ is the lowest eigenvalue of the Hamiltonian.

The mathematical procedure, however, is slightly different if we consider a fixed network of contacts (*quenched* case) or a dynamical pattern, in which contacts evolve at random in time (*annealed* case). We now present the development of the mean-field equations for each case, with particular attention to scale-free networks, in which the heterogeneity of the contacts given by a power-law degree distribution $P(k) \propto k^{-\alpha}$ plays an important role on the criticality of the model.

III. ANNEALED COMPLEX NETWORKS

An annealed network is a time-evolving population in which the contacts between nodes are randomly created and annihilated over time, in such a way that the expected degree (number of contacts) of each node is preserved during the evolution.

The *annealed network approximation* is a simple and very useful tool to study dynamical processes in complex networks [28], and was used to understand the role of complexity in the Ising model [17], the percolation process [26], and epidemic spreading models [12]. It consists into replacing the static (quenched) network of connections by the time-average of a an annealed network, in which the expected degrees of each node are the same as the static version. In spite of correctly predicting the critical behavior of some dynamical processes in static networks, the annealed network approximation can lead to some qualitatively different results. Therefore, for this work, we consider the annealed and quenched cases strictly as different models with their own particular aspects.

An annealed network can be modeled by the following procedure: for each node $i = 1, 2, ..., N$, we first select a random value θ_i from a distribution $p(\theta)$ (once selected, each value remains the same for the rest of the process). We then connect each pair of nodes (i, j) with probability:

$$p_{ij} = \frac{\theta_i \theta_j}{\langle \theta \rangle N} \qquad (3)$$

Where:

$$\langle \theta \rangle = \frac{1}{N} \sum_{i=1}^{N} \theta_i \qquad (4)$$

Is the average of θ_i over the nodes. Each execution of this process results in a fixed network with degree distribution approximately $p(k)$ (the same as the θ_i variables). Consider the ensemble of all possible executions. The annealed network is then constructed by randomly picking samples of this ensemble of networks over time. Therefore, the time average of the annealed network is simply the average over the ensemble. For instance, the degree k_i of node i is a Poisson random variable centered around the expected value $\bar{k}_i = \theta_i$, where the bar indicates the average over time.

In order to obtain an analytical expression for the Bose-Hubbard model in annealed networks, we consider that the time evolution of the network is faster than the typical time scale of the physical model. In this scenario, we can replace the adjacency matrix elements α_{ij} in the Bose-Hubbard Hamiltonian (eq. 1) by the probabilities p_{ij} that each pair of nodes is connected, given by eq. 3. Including also the mean-field assumption from eq. 2, the hopping term becomes:

$$
\begin{aligned}
-t \sum_{i,j} \alpha_{ij} a_i a_j^\dagger &\approx -t \sum_{i,j} \left[\frac{\theta_i \theta_j}{\langle \theta \rangle N} \left(\psi_i a_j + \psi_j a_i^\dagger - \psi_i \psi_j \right) \right] \\
&\approx -\frac{t}{\langle \theta \rangle N} \left[\sum_i a_i^\dagger \theta_i \sum_j \psi_j \theta_j + \right. \\
&\quad + \left. \sum_j a_j \theta_j \sum_i \psi_i \theta_i - \sum_i \psi_i \theta_i \sum_j \psi_j \theta_j \right] \\
&\approx -t\gamma \sum_i \theta_i (a_i^\dagger + a_i) + t\langle \theta \rangle N \gamma^2 \qquad (5)
\end{aligned}
$$

Where we defined the global order parameter as:

$$\gamma = \frac{1}{\langle \theta \rangle N} \sum_i \psi_i \theta_i \qquad (6)$$

Therefore, the mean-field Hamiltonian is site-decoupled as:

$$H_{MF} = \sum_i H_i + t\langle \theta \rangle N \gamma^2 \qquad (7)$$

With the single-site Hamiltonian defined as:

$$H_i = \frac{U}{2} n_i (n_i - 1) - \mu n_i - t\gamma \theta_i (a_i + a_i^\dagger) \qquad (8)$$

For a given distribution $p(\theta)$, the Hamiltonian is a function of γ, which must be determined by minimizing the fundamental energy. As mentioned, we focus on scale-free networks, for which the degree distribution is a power-law:

$$p(\theta) = A\theta^{-\alpha}, \quad \alpha > 0 \qquad (9)$$

Where A is the convenient normalization constant. Numerical methods can be used to find the fundamental state and the zero-temperature value of the order parameter γ as a function of t, μ and U.

A. Numerical solution of the annealed mean-field model

Knowing the distribution θ_i, the mean-field Hamiltonian H_{MF} is a function of a single scalar variable, the order parameter γ. The zero-temperature value of γ is that for which the fundamental state energy (i.e., the lowest eigenvalue of H_{MF}) is minimal. For a given γ, the lowest eigenvalue of H_{MF} is the sum of the lowest eigenvalues of H_i for each site i plus the constant $\langle \theta \rangle N \gamma^2$.

Notice that the single-site Hamiltonian is, in the boson number basis $\{|n\rangle\}$, an infinite symmetric tridiagonal matrix, whose main diagonal elements are $\langle n|H_i|n\rangle = Un(n-1)/2$ and the off-diagonal elements are $\langle n|H_i|n-1\rangle = \langle n-1|H_i|n\rangle = -t\gamma\theta_i\sqrt{n}$, all the other elements being zero. As the diagonal elements increase faster with n than the off-diagonal ones, we expect that high-n elements should not contribute to the lowest eigenvalue of H_i. Physically, this is equivalent to affirm that high occupation number states do not contribute to the fundamental eigenstate. We can, therefore, truncate the matrix at a sufficient order n_{max} and use numerical diagonalization to find the lowest eigenvalue of each site (and thus of the whole system) as a function of γ. Finally, a scalar minimization procedure can be used to find the value of γ that minimizes the fundamental state energy.

By repeating this procedure for different values of t/U and μ/U (the Hamiltonian is scalable by U), we can construct a phase diagram for the superfluid order parameter γ. Figure 1 shows the numerically determined value of γ, exhibiting the quantum phase transition between a Mott insulating phase ($\gamma = 0$) and a superfluid phase ($\gamma \neq 0$). For the numerical diagonalization of H_i, the matrix is truncated at $n_{max} = 100$, which we verified to be far
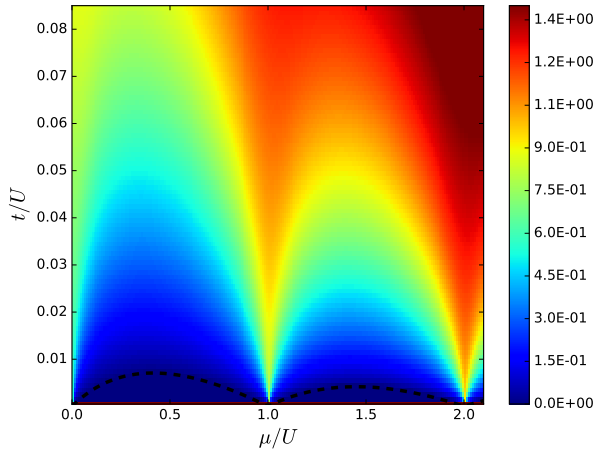
FIG. 1. Global order parameter γ as a function of the relative hopping t/U and chemical potential μ/U, for a scale-free distribution of $N = 1000$ sites with power-law exponent $\alpha = 2.5$. The dashed line is the transition curve between the Mott insulator ($\gamma = 0$) and the superfluid ($\gamma \neq 0$) phase, as predicted by eq. 17.

above the limit at which the results do not change with n_{max}.

Figure 1 shows the first two of the so called *Mott lobes* [40], inside which the number of particles per site is a well-defined quantum number. The dashed lines are the edges of the Mott lobes, defined by the superfluid/insulator phase transition. A precise expression for the mean-field critical curve can be found using perturbation theory.

B. Analytical expression for the insulator/superfluid phase transition

Close to the phase transition, we expect that the value of the order parameter γ is either zero or very small. Therefore, one can analyze the site-Hamiltonian (eq. 8) perturbatively with respect to $t\gamma\theta_i$.[41]

Rewriting eq. 8 as:

$$H_i = H_i^{(0)} - \gamma V_i \tag{10}$$

Where:

$$H_i^{(0)} = \frac{U}{2} n_i(n_i - 1) - \mu n_i \tag{11}$$

$$V_i = t\theta_i(a_i + a_i^\dagger) \tag{12}$$

The unperturbed Hamiltonian (eq. 11) corresponds to the so called atomic limit of the Bose-Hubbard model [42], which is diagonal in the occupation number basis $\{|n_i\rangle\}$ and has eigenvalues given by $E^{(0)}(n) =$

$(U/2)n(n-1) - \mu n$. The eigenstate of $H_i^{(0)}$ with lowest eigenvalue is $|n^*\rangle$, where $n^* = \lceil \mu/U \rceil$ (the lowest integer greater or equal to μ/U) if $\mu > 0$ and $n^* = 0$ if $\mu < 0$.

The first order correction from the perturbation V_i is zero, because it does not preserve particle number. The second order correction is then:

$$E_i^{(2)} = \gamma^2 \sum_{n \neq n^*} \frac{|\langle n|V_i|n^*\rangle|^2}{E^{(0)}(n^*) - E^{(0)}(n)}$$

$$= \gamma^2 t^2 \theta_i^2 \left(\frac{n^*}{U(n^*-1) - \mu} + \frac{n^*+1}{\mu - Un^*} \right) \tag{13}$$

Using that $n^* = \lceil \mu/U \rceil$ for $\mu > 0$, define the functions:

$$f(x) = \frac{1}{2} \lceil x \rceil \lfloor x \rfloor - x \lceil x \rceil \tag{14}$$

$$g(x) = \frac{\lceil x \rceil}{x - \lfloor x \rfloor} + \frac{\lceil x \rceil + 1}{\lceil x \rceil - x} = \frac{x + 1}{(\lfloor x \rfloor - x)(x - \lceil x \rceil)} \tag{15}$$

Then the system ground state energy can be written, up to second order, as:

$$E_{GS} = \sum_i \left\{ Uf\left(\frac{\mu}{U}\right) - \frac{\gamma^2 t^2 \theta_i^2}{U} g\left(\frac{\mu}{U}\right) \right\} + \gamma^2 tN\langle\theta\rangle$$

$$= N\left\{ Uf\left(\frac{\mu}{U}\right) + \gamma^2 \left[\frac{-t^2 \langle\theta^2\rangle}{U} g\left(\frac{\mu}{U}\right) + t\langle\theta\rangle \right] \right\} \tag{16}$$

The mass term (the coefficient that multiplies γ^2 in eq. 16) defines the stability of the $\gamma = 0$ solution. Making the mass term equal to zero defines the quantum phase transition. For the hopping term, this condition can be written as:

$$t_c = \frac{U}{g(\mu/U)} \frac{\langle\theta\rangle}{\langle\theta^2\rangle} \tag{17}$$

If $t > t_c$, the system is a superfluid, whereas $t < t_c$ defines the Mott insulator phase. In figure 1, the dashed line represents the phase transition curve, calculated by eq. 17 and using $\langle\theta\rangle/\langle\theta^2\rangle$ from the power-law distribution. The analytical expression for the critical curve is in good agreement with the numerical results.

A remarkable fact for scale-free networks (whose degree distribution satisfy eq. 9) is that, for large population sizes N and assuming that the maximum degree scales with N (i.e, $\max\{\theta_i\} \sim N$), the second moment $\langle\theta^2\rangle$ diverges for any power-law exponent α that satisfies $\alpha \leq 3$. In particular, the quantity $\langle\theta\rangle/\langle\theta^2\rangle$ (which is the inverse of the so called *complexity* of the network [2]) scales as $\sim N^{-1}$ for $0 < \alpha \leq 2$, as $\sim N^{-(3-\alpha)}$ for $2 < \alpha < 3$ and as $\sim 1/\ln N$ for $\alpha = 3$. Therefore, for such networks, the critical hopping term t_c becomes smaller as N increases, going to zero at the thermodynamic limit, meaning that no Mott insulator can be observed in such

(a)$\alpha = 2.5$ (b)$\alpha = 3.2$
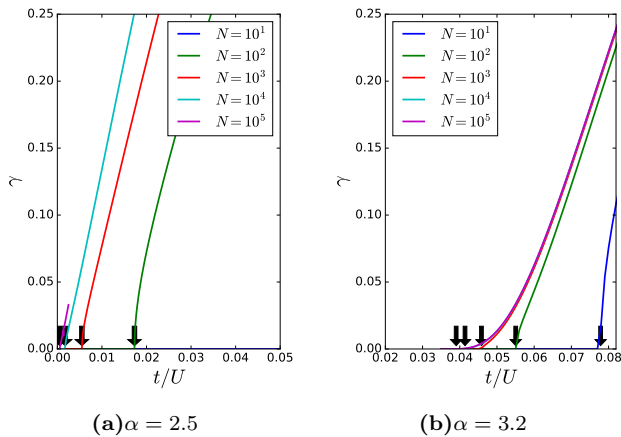
FIG. 2. Global order parameter γ as a function of the relative hopping term t/U, for different population sizes N. In figure (a), the critical point goes asymptotically to zero as N increases, because the power-law exponent is $\alpha = 2.5 < 3$. In figure (b), for which $\alpha = 3.2 > 3$, the critical point remanis finite. The black arrows indicate the values of t_c as predicted by eq. 17. All numerical results use $n_{max} = 100$.

a condition. This result is strongly analogous to that for epidemic spreading in scale-free networks, for which the critical point of an epidemic outbreak is also proportional to the inverse of the complexity, meaning that no healthy phase is observed at the thermodynamic limit [12, 43]. Further discussion about the meaning of this curious result is given in section V.

This effect can be observed in our model by comparing the quantum critical point for annealed networks with same exponent α and increasing population size N. Figure 2 shows the phase diagram for fixed μ and U, showing the order parameter as a function of the hopping energy t. The curves are plotted for different population sizes from 10 to 10^4 and for two values of the power-law exponent α. Notice that, for $\alpha = 2.5$, the critical point goes to zero as N increases, whereas it approaches a finite value for $\alpha = 3.2$. The analytical prediction from eq. 17 is indicated by the black arrows, for comparison with numerical data.

Annealed networks provides us a simple framework to capture the essential influence of a heterogeneous contact structure in our model. However, greater complexity is considered by studying the model in static (quenched) networks, which may present many other features and correlations that were rejected in the annealed model. Moreover, with a static network formalism, one can recover the individual site information of the field ψ, which was lost in the annealed approximation and replaced by the global order parameter γ.

IV. QUENCHED COMPLEX NETWORKS

We refer as *quenched* a network whose connections are static over time. A quenched theory over a network must consider its whole contact structure. Therefore, along this section, we do not replace the adjacency matrix elements by an average value or probability as done in section III.

One can still simplify the Bose-Hubbard Hamiltonian using the mean-field approximation from eq. 2, with the following procedure:

$$
\begin{aligned}
-t\sum_{i,j}\alpha_{ij}a_i a_j^\dagger &\approx -t\sum_{i,j}\left[\alpha_{ij}\left(\psi_i a_j + \psi_j a_i^\dagger - \psi_i\psi_j\right)\right] \\
&\approx -t\bigg[\sum_i a_i^\dagger \sum_j \alpha_{ij}\psi_j + \\
&\quad + \sum_j a_j \sum_i \alpha_{ij}\psi_i - \sum_i \psi_i \sum_j \alpha_{ij}\psi_j\bigg] \\
&\approx -t\sum_i \varphi_i(a_i^\dagger + a_i) + t\sum_i \varphi_i\psi_i \quad (18)
\end{aligned}
$$

Where we used the symmetry of the adjacency matrix to flip the indexes i, j in one of the terms, and defined the sum of the field ψ_i over the neighbors of site i (represented as $\aleph(i)$) as:

$$
\varphi_i = \sum_j \alpha_{ij}\psi_j = \sum_{j\in\aleph(i)} \psi_j \qquad (19)
$$

The Hamiltonian is then decoupled in single site terms:

$$
H = \sum_i H_i,
$$

$$
H_i = \frac{U}{2}n_i(n_i-1) - \mu n_i - t\varphi_i(a_i^\dagger + a_i) + \varphi_i\psi_i \qquad (20)
$$

Which can be numerically diagonalized as a function of each value of φ_i with the same procedure explained in section III A.

A. Numerical solution for the quenched network case

For the case of annealed networks, we have reduced the problem of finding the correct mean-field parameters to a scalar minimization problem, i.e., minimizing the total Hamiltonian of eq.7 with respect to the global order parameter γ, getting rid of all the local information ψ_i. For the quenched case, each single-site Hamiltonian H_i depends on the value of the local (ψ_i) and neighboring (ϕ_i) fields. A drawback is that the total ground state energy (given by the sum over each local ground state energy) is not bounded by below, meaning that a minimization process would fail to determine the correct ψ_i values.

Therefore, in this case, we must use a self-consistency rule to solve the mean-field problem. Such rule is obtained from the definition of the mean-field $\psi_i = \langle a_i \rangle$ (recall eq. 2). For zero temperature, the average $\langle a_i \rangle = \langle GS | a_i | GS \rangle$ is the expected value of the operator in the system's ground state. As the global Hamiltonian is site-decoupled, one can write the total system ground state as:

$$|GS\rangle = |u_1\rangle \otimes |u_2\rangle \otimes ... \otimes |u_N\rangle \qquad (21)$$

Where $|u_i\rangle$ is the fundamental eigenstate of H_i, i.e., such that $H_i |u_i\rangle = \epsilon_i^0 |u_i\rangle$ and ϵ_i^0 is the lowest eigenvalue. We can expand $|u_i\rangle$ in the basis of occupation number states $\{|n\rangle\}$:

$$|u_i\rangle = \sum_{n=0}^{\infty} \beta_i^n |n\rangle, \quad \beta_i^n = \langle n | u_i \rangle \qquad (22)$$

Where we removed the site index i from the boson number states $|n\rangle$ to avoid loading the notation. The field ψ_i can now be written in terms of the coefficients β_i^n:

$$\psi_i = \langle u_i | a_i | u_i \rangle = \sum_{n=0}^{\infty} \bar{\beta}_i^n \beta_i^{n+1} \sqrt{n+1} \qquad (23)$$

As explained in section III A, one can truncate the Hamiltonian H_i up to $n = n_{max}$ and numerically determine the lowest eigenvalue ϵ_i^0 and its eigenvector $|u_i\rangle$. The normalized coefficients of $|u_i\rangle$ then give us the values of β_i^n, for $n = 0, 1, ..., n_{max}$. Notice, however, that H_i depends on the neighboring field $\varphi_i = \sum_j \alpha_{ij} \psi_j$, and so do the β_i^n coefficients. Therefore, eq. 23 is a (non-linear) self-consistency relation for the field ψ_i. Starting from an initial set of values, one can use this equation to iteratively find the physical solution of the system by the fixed-point method (i.e., calculating the RHS with the current ψ values and updating them with the results until the values stop changing).

Once the physical solution is found, the global order parameter γ can be calculated by eq. 6, replacing θ_i and $\langle \theta \rangle$ respectively by the site degree k_i and its average $\langle k \rangle$ over the network, thus $\gamma = 1/(N\langle k \rangle) \sum_i k_i \theta_i$. Figure 3 shows the phase diagram for a quenched scale-free network with $N = 1000$ sites, minimum degree $k_{min} = 4$ and power-law exponent $\gamma = 2.5$. The network is generated by the configuration model [1], by which random connections are established according to a predefined degree sequence.

The iterative version of eq. 23 defines a discrete dynamical process. The stability of the trivial solution $\psi_i = 0$, $i = 1, 2, ..., N$ can be determined by perturbation theory over H_i, which provides the boundary of the Mott insulator phase in the quenched model.
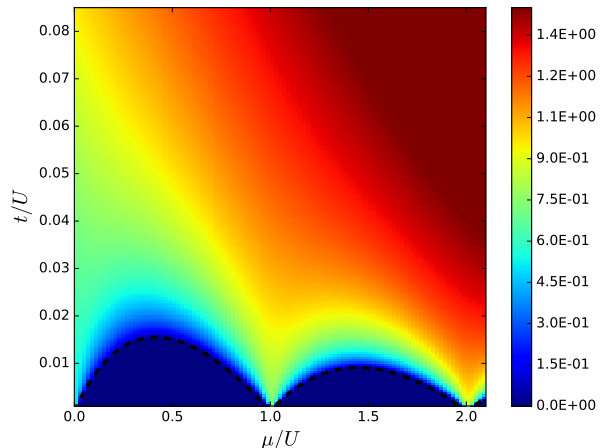
FIG. 3. Phase diagram of the global order parameter γ as a function of the relative hopping t/U and chemical potential μ/U, for a scale-free quenched network of $N = 1000$ sites, minimum degree $k_{min} = 4$ and power-law exponent $\alpha = 2.5$. The dashed line is the transition between the Mott insulator ($\gamma = 0$) and the superfluid ($\gamma \neq 0$) phase, according to the quenched model prediction (eq. 31).

B. Quenched critical point by perturbation theory

Assuming that the neighboring field φ_i is small for every site i, we write the single-site Hamiltonian as an unperturbed term plus a perturbation proportional to φ_i:

$$H_i = H_i^{(0)} + V_i + t\varphi_i \psi_i \qquad (24)$$
$$H_i^{(0)} = \frac{U}{2} \hat{n}(\hat{n} - 1) - \mu \hat{n} \qquad (25)$$
$$V_i = -t\varphi(\hat{a} + \hat{a}^\dagger) \qquad (26)$$

Where in RHS of eqs. 25 and 26 we dropped the site index i to simplify the notation for the next equations (thus $\hat{n} = n_i$, $\varphi = \varphi_i$ and $\hat{a} = a_i$). As in the annealed case, the first order energy correction of H_i vanishes, because the perturbation V_i does not preserve the particle number. However, the eigenstates have a finite correction at the first order, whereas it can be shown that the second order correction is null. In particular, for the fundamental state eigenvector $|u\rangle$ (originally $|u_i\rangle$), the first order correction is [44]:

$$|u\rangle \approx |n^*\rangle + |u^{(1)}\rangle$$
$$|u^{(1)}\rangle = -\sum_{n \neq n^*} \frac{\langle n | -t\varphi(\hat{a} + \hat{a}^\dagger)|n^*\rangle}{E^{(0)}(n) - E^{(0)}(n^*)} |n\rangle \qquad (27)$$

Where, as defined in section III B, $E^{(0)}(n) = (U/2)n(n-1) - \mu n$, $n^* = 0$ if $\mu < 0$ and $n^* = \lceil \mu/U \rceil$ if $\mu > 0$, thus $|n^*\rangle$ is the unperturbed fundamental state.

The only non-vanishing terms in summation from eq. 27 are those for which $n = n^* \pm 1$, yielding:

$$|u^{(1)}\rangle = t\varphi \left[\frac{\sqrt{n^*}\,|n^*-1\rangle}{U(n^*-1)-\mu} + \frac{\sqrt{n^*+1}\,|n^*+1\rangle}{\mu-Un^*} \right] \quad (28)$$

We can now use the first order correction of $|u\rangle$ to expand the average $\langle \hat{a} \rangle$, which is used to calculate ψ_i by iteration:

$$\langle u|\hat{a}|u\rangle \approx t\varphi \left[\frac{n^*}{U(n^*-1)-\mu} + \frac{n^*+1}{\mu-Un^*} \right] = \frac{t\varphi}{U} g\!\left(\frac{\mu}{U}\right) \quad (29)$$

Where we used the definition of $g(x)$ from eq. 15. Therefore, for small φ_i (putting back the omitted site index i), the self-consistency rule (eq. 23) for the field ψ_i becomes:

$$\psi_i \approx \frac{tg(\mu/U)}{U}\varphi_i = \frac{tg(\mu/U)}{U} \sum_j \alpha_{ij}\psi_j \quad (30)$$

This is the linear expansion of the dynamical process defined by iterating eq. 23. The stability condition of the trivial solution $\psi_i = 0\,\forall i$ is that all eigenvalues of the Jacobian of the map (which is given by the matrix elements $t\,g(\mu/U)\alpha_{ij}/U$) are less than 1. Therefore, denoting by Λ the maximal eigenvalue of the adjacency matrix α_{ij}, the Mott insulator phase is stable if:

$$\frac{t\,g(\mu/U)}{U}\Lambda < 1 \implies t_c = \frac{U}{g(\mu/U)}\frac{1}{\Lambda} \quad (31)$$

For a network with power-law degree distribution $P(k) \propto k^{-\alpha}$, the large-N scaling of the maximal eigenvalue Λ of the adjacency matrix was determined by Chung *et al.* [45], for a very general class of graphs, to be:

$$\Lambda \sim \max\left[\sqrt{k_{max}}, \frac{\langle k^2 \rangle}{\langle k \rangle} \right] \quad (32)$$

Independently of the convergence of the second moment $\langle k^2 \rangle$, Λ increases with k_{max}. Therefore, the critical hopping term t_c vanishes at the thermodynamic limit, provided that for $N \to \infty$ the maximal degree k_{max} scales with some positive power of N. This is independent of the power-law exponent α. For $\alpha > 3$, then, the quenched and annealed cases diverge from one another, as the annealed model predicts a finite non-null critical point. In the context of epidemic models, such divergence between the two formulations was already widely discussed [46–48], and its physical origin is related to the role of the hubs (most connected sites) and *k-cores* [49] (low-connected populations of nodes) into triggering activity on the network [50].

Although the study of the global order parameter γ and the critical point t_c provides some understanding on how the heterogeneity of contacts affects the Bose-Hubbard model, more knowledge can be extracted by analyzing the local field ψ_i.

C. Local field analysis: eigenvector centrality

In the science of complex networks, there is a wide variety of metrics that reduce the complicated information of the network structure into some scalar measures, which try to capture fundamental aspects both in local and global scale [1, 3]. One of the most important class of such measures is the set of *centrality* metrics, which attempt to classify the importance of each node (site) in the network. The notion of *importance* of a node is specific from each centrality metric.

Numerical solution of eq. 23 provides the value of ψ_i for each site $i = 1, 2, ..., N$. One should expect that more "important" sites may have greater values of ψ_i than less "important" ones. This can be verified by comparing each value of ψ_i with some centrality metric of the node i, and then verify if there is a good correlation.

The simplest centrality measure is the degree k_i itself, i.e., the number of connections that site i has. Indeed, nodes with many connections (hubs) are, in general, very important for most dynamical processes in networks. For this work, we also present the *eigenvector centrality* metric [51]. The basic idea of this metric is that nodes which are linked to other important nodes are also important. In other words, the importance of a node is proportional to the importance of its neighbors [1]. This intuitive idea defines a recursive relation which can be expressed as an eigenvalue equation with the adjacency matrix of the network:

$$\lambda x_i = \sum_j \alpha_{ij} x_j \quad (33)$$

Motivated by this, the eigenvector centrality of a node i is defined as the corresponding entry x_i of the eigenvector $\mathbf{x}$ with highest eigenvalue $\lambda = \Lambda$ (preferably, $\mathbf{x}$ should be normalized).

Recall that, when deducing the critical point of the quenched model, we wrote the linearized version of the update rule, eq. 30, which is precisely an eigenvalue equation for the adjacency matrix. Therefore, when the system is close to the phase transition, one should expect a great correlation between the eigenvector centrality and the value of the local field ψ_i. On the other hand, this idea can also be used to detect the critical point when simulating the model with different parameters.

In figures 4, 5 we show scatter plots of the local field ψ versus the degree and eigenvector centralities, respectively, for the same scale-free network used in figure 3. From the upper to the lower plot, the hopping term is
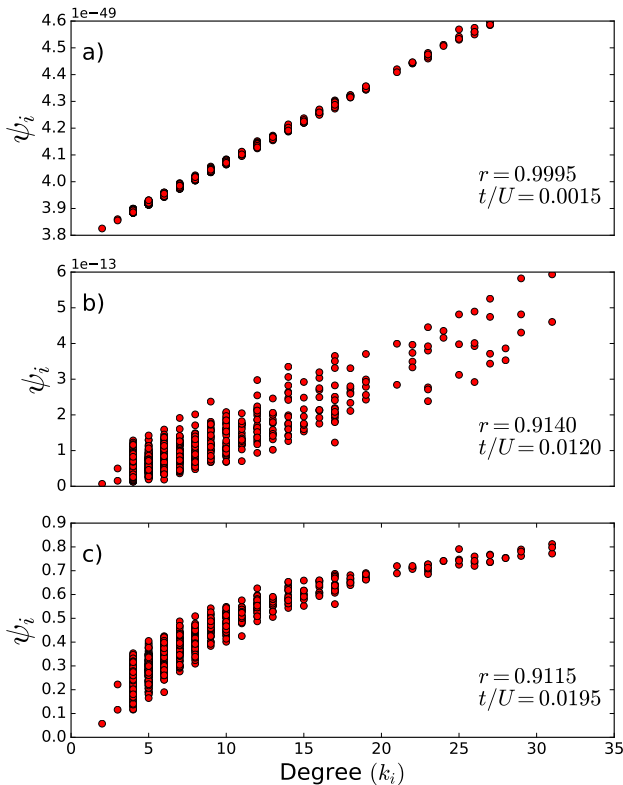
FIG. 4. Local field ψ_i and the degree k_i of each node, for a a) subcritical, b) critical and c) supercritical system, for the Bose-Hubbard model in the same network used in figure 3. The chemical potential is $\mu/U = 0.2$ in all plots, and the critical point, according to eq. 31, is $t_c/U \approx 0.01203$ for this network. The vertical axis is scaled, in each plot, for better visualization of the data.

a) subcritical $(t < t_c)$, b) critical $(t \approx t_c)$ and c) supercritical $(t > t_c)$. We also show the Pearson's correlation coefficient for each set of values, denoted as r on the plots. For the plots a) and b), the order parameter is essentially null $(\psi_i = 0, \forall i)$, so the field values are unphysical remainings of the numerical procedure (notice the powers of ten above each plot). In the critical case (plot b)), the correlation between ψ_i and the eigenvector centrality x_i is, up to the 4th decimal place of the Pearson's coefficient, equals to 1. This is a consequence of eq. 30, which shows that the system can be approximated to a linear dynamical process around the phase transition. Therefore, close to the critical point, the eigenvector centrality is the most precise centrality measure to describe the site-specific activity, as the calculation of x_1 and the solution of eq. 23 represent essentially the same process.

We finally show the dependence of the correlation coefficient r (between the centrality measure and the local field ψ_i) with the hopping term t when crossing the insulator/superfluid phase transition. For both degree and eigenvector centrality metrics, the behavior of the correlation is singular at the phase transition (represented
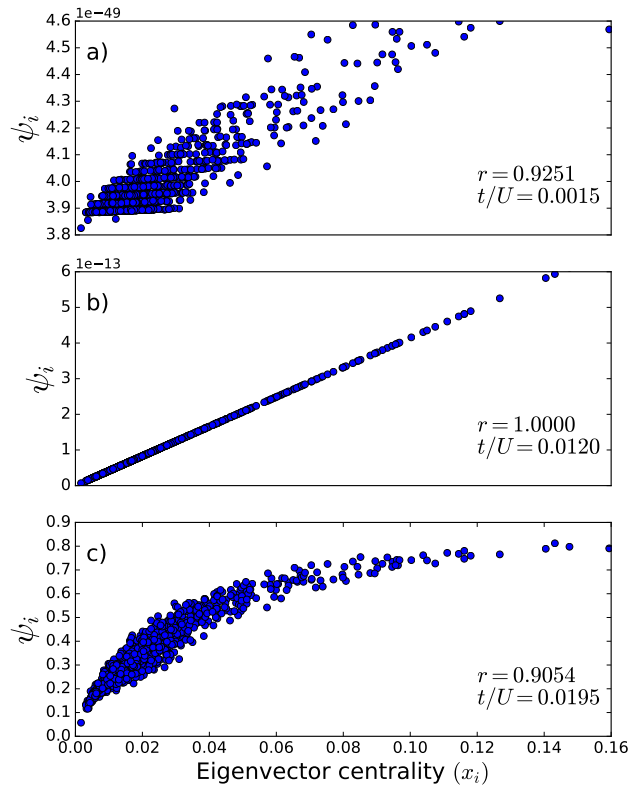
FIG. 5. Local field ψ_i and the eigenvector centrality x_i of each node, for a a) subcritical, b) critical and c) supercritical system, for the Bose-Hubbard model in the same network used in figure 3. Data is the same as in the previous figure.

by the dashed line), but the eigenvector centrality clearly shows better correlation around the transition. However, for largest values of the hopping term t, the degree overcomes the eigenvector centrality and becomes more correlated to the local field. It is important to notice that, at the left of the transition, the field is essentially zero, and therefore the correlations at this region relate only with the remainings of the numerical method. Yet, using correlation between the local field and centrality measures is a good method to numerically identify the phase transition between the Mott insulator phase and the superfluid phase.

V. LIMITATIONS OF THE MEAN FIELD: BOSE GLASS PHASE

The numerical calculations performed in this work are inside the scope of the mean-field Bose-Hubbard model. The analytical method that we used predicts exactly the mean-field critical point (which however may differ from the exact value of the model).

The mean-field approach neglects quantum fluctuations around the expected values of the quantum operators a_i and $a_i^\dagger$. Due to this crude approximation, an im-
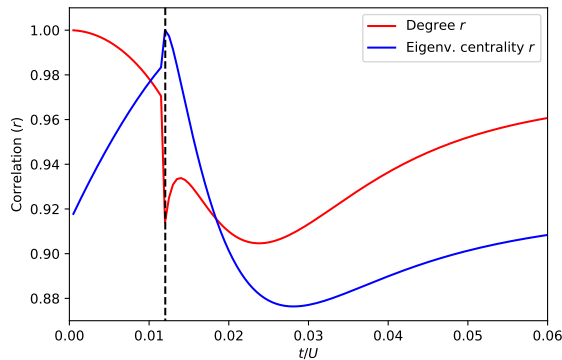
FIG. 6. Pearson's r coefficient between the local field ψ_i and the degree (red) and eigenvector (blue) centrality measures, as a function of the relative hopping term. The critical point, as predicted by eq. 31, is shown as a dashed black line. The chemical potential is $\mu/U = 0.2$, and the network is the same as used in figure 3.

portant phenomenon may be lost: the *Bose glass* phase, described by Fisher *et. al.* [38], which occurs as an intermediate phase between the Mott insulator and the superfluid phases (therefore, for intermediate values of the hopping term t). It is characterized by the absence of gap for adding or removing particles (which is a characteristics of a superfluid), but a zero global order parameter (which is characteristic from the Mott insulator phase). The system has diverging superfluid susceptibility but finite compressibility [38]. The Bose glass is considered a Griffiths phase, in analogy to a similar result with the ferromagnetic Ising model obtained by Griffiths [52] in 1969.

In regular lattices, the Bose glass phase appears when random disorder is introduced on the model (for example, at the chemical potential). It would also be expected to appear for complex networks, which naturally presents disorder by the heterogeneity of contacts between sites. However, further study would be necessary to prove this from our model.

An important consequence lies at our claim that the model critical point vanishes for scale-free networks in the thermodynamic limit. We can speculate that the inhomogeneous topology of a complex network produces a Bose glass phase, and that the phase transition that we were able to predict is actually between the Mott insulator and the Bose glass phase. We also speculate that the critical point between the Bose glass and superfluid phases actually remains finite (non-vanishing) at the thermodynamic limit. Indeed, in Fisher's work, it is shown that, if the disorder in the chemical potential is sufficiently high (or unbound), the Mott insulator phase disappears, yet the Bose glass persists. Our claim is also based on recent works with the contact process [53] and epidemic models [54–56], which show that both quenched

and annealed mean-field theories can predict the "dirty" transition, but not the existence of a Griffiths phase, in which there is activity localized around the hubs. Computational evidence suggest that the transition between the Griffiths and the global active phase remains finite at the thermodynamic limit [56]. For the Bose-Hubbard model in complex networks, however, further work is demanded to test our proposals.

VI. CONCLUSIONS

We have studied the Bose-Hubbard model under mean-field hypothesis, for sites that connect to each other as a complex network structure. The mean-field assumption decouples the Hamiltonian in independent components for each site, allowing analytical and numerical treatment even in the lack of translational symmetry present in the complex network. For the annealed network case, we can find the global superfluid order parameter γ by minimizing the total energy with respect to it. For the quenched case, we find the local field parameter ψ_i for each site i by numerically solving the restriction rule imposed by eq. 23. In both cases, we use our numerical solution to trace the t versus μ phase diagram for the global order parameter. Using perturbation theory (which becomes exact in the critical point), we can analytically calculate the phase transition curve for both quenched and annealed formulations, which show good agreement with the numerical data.

The mean-field approach predict some dramatic consequences for the networks with diverging second degree moment $\langle k^2 \rangle$ or maximal degree k_{max} in the thermodynamic limit, as already observed for several other models. However, as discussed, we must be careful at the interpretation of our results, as we did not consider the existence of a Bose glass phase during our analysis. Yet, the inexistence of the Mott insulator phase (giving place to the Bose glass) in scale-free topology may be physical, although further study should be done on the subject. This may have relevant consequences, allowing, for example, the production of a Bose glass in networks with low tunnelling amplitudes. The recent development of engineered optical potentials opens the possibility of experimental realization of complex topologies for bosons, and consequently the application of our findings.

ACKNOWLEDGMENTS

[1] M. Newman, *Networks: An Introduction* (Oxford university press, 2010).

[2] S. Boccaletti, V. Latora, Y. Moreno, M. Chavez, and D.-U. Hwang, Physics reports **424**, 175 (2006).

[3] A.-L. Barabási *et al.*, *Network science* (Cambridge university press, 2016).

[4] L. da Fontoura Costa, O. N. O. Jr., G. Travieso, F. A. Rodrigues, P. R. V. Boas, L. Antiqueira, M. P. Viana, and L. E. C. Rocha, Advances in Physics **60**, 329 (2011), https://doi.org/10.1080/00018732.2011.572452.

[5] A.-L. Barabási and R. Albert, science **286**, 509 (1999).

[6] D. J. Watts and S. H. Strogatz, nature **393**, 440 (1998).

[7] H. Jeong, S. P. Mason, A.-L. Barabási, and Z. N. Oltvai, Nature **411**, 41 (2001).

[8] R. Sharan and T. Ideker, Nature biotechnology **24**, 427 (2006).

[9] J. Wang and P. De Wilde, Physical Review E **70**, 066121 (2004).

[10] F. Morone and H. A. Makse, Nature **524**, 65 (2015).

[11] Y. Moreno, M. Nekovee, and A. F. Pacheco, Physical Review E **69**, 066130 (2004).

[12] R. Pastor-Satorras and A. Vespignani, Phys. Rev. Lett. **86**, 3200 (2001).

[13] M. J. Keeling and K. T. Eames, Journal of the Royal Society Interface **2**, 295 (2005).

[14] R. Pastor-Satorras, C. Castellano, P. Van Mieghem, and A. Vespignani, Reviews of modern physics **87**, 925 (2015).

[15] G. A. Pagani and M. Aiello, Physica A: Statistical Mechanics and its Applications **392**, 2688 (2013).

[16] M. Leone, A. Vázquez, A. Vespignani, and R. Zecchina, The European Physical Journal B - Condensed Matter and Complex Systems **28**, 191 (2002).

[17] G. Bianconi, Physics Letters A **303**, 166 (2002).

[18] L. Jahnke, J. W. Kantelhardt, R. Berkovits, and S. Havlin, Physical review letters **101**, 175702 (2008).

[19] M. Sade, T. Kalisky, S. Havlin, and R. Berkovits, Physical Review E **72**, 066123 (2005).

[20] B. J. Kim, H. Hong, P. Holme, G. S. Jeon, P. Minnhagen, and M. Choi, Physical Review E **64**, 056135 (2001).

[21] A. M. Souza and H. Herrmann, Physical Review B **75**, 054412 (2007).

[22] R. Burioni, D. Cassi, M. Rasetti, P. Sodano, and A. Vezzani, Journal of Physics B: Atomic, Molecular and Optical Physics **34**, 4697 (2001).

[23] I. Brunelli, G. Giusiano, F. Mancini, P. Sodano, and A. Trombettoni, Journal of Physics B: Atomic, Molecular and Optical Physics **37**, S275 (2004).

[24] I. de Oliveira, F. de Moura, M. Lyra, J. Andrade Jr, and E. Albuquerque, Physical Review E **81**, 030104 (2010).

[25] M. Barahona and L. M. Pecora, Physical review letters **89**, 054101 (2002).

[26] R. Cohen, K. Erez, D. ben Avraham, and S. Havlin, Phys. Rev. Lett. **85**, 4626 (2000).

[27] G. Bianconi, Journal of Statistical Mechanics: Theory and Experiment **2012**, P07021 (2012).

[28] S. N. Dorogovtsev, A. V. Goltsev, and J. F. F. Mendes, Rev. Mod. Phys. **80**, 1275 (2008).

[29] D. Jaksch, C. Bruder, J. I. Cirac, C. W. Gardiner, and P. Zoller, Phys. Rev. Lett. **81**, 3108 (1998).

[30] F. Cataliotti, S. Burger, C. Fort, P. Maddaloni, F. Minardi, A. Trombettoni, A. Smerzi, and M. Inguscio, Science **293**, 843 (2001).

[31] W. Zwerger, Journal of Optics B: Quantum and Semiclassical Optics **5**, S9 (2003).

[32] R. Ketterer, P. C. V. da Silva, L. F. Santana, and S. R. Muniz, in *Latin America Optics and Photonics Conference* (Optical Society of America, 2012) p. LM1B.3.

[33] A. L. Gaunt and Z. Hadzibabic, Scientific reports **2**, 721 (2012).

[34] J. G. Lee and W. Hill III, Review of Scientific Instruments **85**, 103106 (2014).

[35] H. A. Gersch and G. C. Knollman, Phys. Rev. **129**, 959 (1963).

[36] D. Jaksch and P. Zoller, Annals of physics **315**, 52 (2005).

[37] I. Bloch, Nature physics **1**, 23 (2005).

[38] M. P. A. Fisher, P. B. Weichman, G. Grinstein, and D. S. Fisher, Phys. Rev. B **40**, 546 (1989).

[39] K. Sheshadri, H. Krishnamurthy, R. Pandit, and T. Ramakrishnan, EPL (Europhysics Letters) **22**, 257 (1993).

[40] P. Buonsante and A. Vezzani, Phys. Rev. A **70**, 033608 (2004).

[41] Indeed, the perturbation $t\gamma\theta_i(a_i + a_i^\dagger)$ is asymptotically close to zero when approaching the critical point, and therefore the expression obtained by perturbation theory is exact (inside the mean-field framework).

[42] V. Rousseau, M. Rigol, F. Hébert, D. Arovas, G. Batrouni, and R. Scalettar, in *APS Meeting Abstracts* (2006).

[43] R. Pastor-Satorras and A. Vespignani, Phys. Rev. E **65**, 035108 (2002).

[44] C. Cohen-Tannoudji, B. Diu, and F. Laloe, Quantum Mechanics, Volume 2, by Claude Cohen-Tannoudji, Bernard Diu, Frank Laloe, pp. 626. ISBN 0-471-16435-6. Wiley-VCH, June 1986. , 626 (1986).

[45] F. Chung, L. Lu, and V. Vu, Proceedings of the National Academy of Sciences **100**, 6313 (2003), http://www.pnas.org/content/100/11/6313.full.pdf.

[46] S. C. Ferreira, C. Castellano, and R. Pastor-Satorras, Physical Review E **86**, 041125 (2012).

[47] D. Chakrabarti, Y. Wang, C. Wang, J. Leskovec, and C. Faloutsos, ACM Transactions on Information and System Security (TISSEC) **10**, 1 (2008).

[48] S. Gómez, A. Arenas, J. Borge-Holthoefer, S. Meloni, and Y. Moreno, EPL (Europhysics Letters) **89**, 38009 (2010).

[49] S. B. Seidman, Social networks **5**, 269 (1983).

[50] C. Castellano and R. Pastor-Satorras, Scientific reports **2**, 371 (2012).

[51] P. Bonacich, American journal of sociology **92**, 1170 (1987).

[52] R. B. Griffiths, Physical Review Letters **23**, 17 (1969).

[53] M. A. Muñoz, R. Juhász, C. Castellano, and G. Ódor, Physical review letters **105**, 128701 (2010).

[54] S. C. Ferreira, C. Castellano, and R. Pastor-Satorras, Physical Review E **86**, 041125 (2012).

[55] H. K. Lee, P.-S. Shim, and J. D. Noh, Physical Review E **87**, 062812 (2013).

[56] A. S. Mata and S. C. Ferreira, Physical Review E **91**, 012816 (2015).